

Article

Geothermal Pavements: Experimental Testing, Prototype Testing, and Numerical Analysis of Recycled Demolition Wastes

Behnam Ghorbani ^{1,2}, Arul Arulrajah ^{1,*}, Guillermo A. Narsilio ³, Suksun Horpibulsuk ^{4,5,6,*} and Apinun Buritatum ⁵

¹ Department of Civil and Construction Engineering, Swinburne University of Technology, Melbourne, VIC 3122, Australia

² AECOM Australia, Pavements and Aviation, Melbourne, VIC 3008, Australia

³ Department of Infrastructure Engineering, The University of Melbourne, Parkville, VIC 3010, Australia

⁴ School of Civil Engineering, Suranaree University of Technology, Nakhon Ratchasima 30000, Thailand

⁵ Center of Excellence in Innovation for Sustainable Infrastructure Development, Suranaree University of Technology, Nakhon Ratchasima 30000, Thailand

⁶ Academy of Science, The Royal Society of Thailand, Bangkok 10300, Thailand

* Correspondence: aarulrajah@swin.edu.au (A.A.); suksun@g.sut.ac.th (S.H.)

Abstract: Geothermal pavements have the potential to reduce the pavement surface temperature by circulating fluid in pipes within the pavement structure. This research investigated an innovative geothermal pavement system with multiple benefits, such as reducing the surface temperature and harvesting heat energy for power generation. This research aimed to provide an understanding of the mechanical properties of geothermal pavements constructed with construction and demolition (C&D) waste materials through large-scale physical testing, experimental testing, small-scale prototype testing, and numerical simulation. The mechanical properties of the geothermal pavement system were assessed under long-term traffic loading conditions using a prototype test system. The repeated load triaxial and repeated-load California bearing ratio tests were also undertaken to evaluate the effect of pipe inclusion on the permanent deformation, stiffness, and strength of the pavement base. A numerical model was subsequently developed and calibrated using the data from small-scale prototype testing. In addition, the effects of the flow rate and pipe materials on the thermal performances of the geothermal pavements were also investigated in this research. The inclusion of pipes in the pavement base layer was found to have negligible detrimental effects on the deformation behavior of RCA. The resilient moduli of recycled concrete aggregate (RCA) samples slightly decreased with the inclusion of pipes. An HDPE pipe reduced the stiffness of the RCA + HDPE mix. On the other hand, a copper pipe's high stiffness improved the mix's strength. The numerical simulations indicated that for the HDPE pipe, increasing the flow rate from 500 mL/min to 2000 mL/min reduced the surface temperature by approximately 1.3%, while using the copper pipe resulted in an approximately 4% further decrease in the surface temperature compared to the HDPE pipe.

Keywords: ground improvement; pavement geotechnics; geothermal pavements; demolition waste; recycled wastes



Citation: Ghorbani, B.; Arulrajah, A.; Narsilio, G.A.; Horpibulsuk, S.; Buritatum, A. Geothermal Pavements: Experimental Testing, Prototype Testing, and Numerical Analysis of Recycled Demolition Wastes. *Sustainability* **2023**, *15*, 2680. <https://doi.org/10.3390/su15032680>

Academic Editor: Hamzeh F. Haghshenas

Received: 20 December 2022

Revised: 30 January 2023

Accepted: 31 January 2023

Published: 2 February 2023



Copyright: © 2023 by the authors. Licensee MDPI, Basel, Switzerland. This article is an open access article distributed under the terms and conditions of the Creative Commons Attribution (CC BY) license (<https://creativecommons.org/licenses/by/4.0/>).

1. Introduction

Asphalt surfaces absorb significant amounts of solar radiation during hot summer days, increasing the pavement surface temperature by up to 70 °C [1]. High temperatures are an important contributor to pavement distresses, such as rutting and cracking, leading to serviceability and stability problems [2,3]. To mitigate these issues, pavement cooling technologies using circulating fluid in pipes at a shallow depth in the pavement surface have been introduced as effective solutions [4–6]. Due to the stress concentration around the pipe, the installation of the pipe in the surface layer requires a special construction technique to prevent pavement surface cracking [5]; hence, this was not attempted in this

research study, which focused specifically on the performances of pipes in the pavement base layer.

Geothermal pavements are formed by embedding pipes in the pavement's granular base layer, which is an efficient method for reducing the pavement surface temperature [7]. In addition, embedding pipes in the granular pavement base layer rather than in the pavement surface layer can result in significant pavement maintenance cost savings. The fluid circulation within the pipes can reduce the surface temperature and subsequently reduce the urban island heat effect. The improved heat transfer properties of pavement base materials, due to their higher resistance to binder degradation against heat energy, are important parameters affecting the service life [3]. In addition, embedding pipes in the granular layers of the pavements rather than the pavement surface layers can result in significant savings in terms of pavement maintenance costs.

Construction and demolition (C&D) materials have emerged as sustainable materials for civil engineering works, particularly in pavement granular base layers. It is well established that C&D materials have similar and in some cases superior deformation responses compared to natural aggregates [8–10]. The utilization of C&D materials in the infrastructure application is considered a sustainable solution to minimize the conventional disposal of C&D waste. In Australia, an enormous quantity of C&D waste, approximately 8.7 million tons of RCA, 1.3 million tons of CB, and 1.2 million tons of RAP, is stockpiled annually and promises to increase continuously [11]. Therefore, various pavement engineering research has attempted to maximize the application of C&D materials as an alternative to the utilization of natural aggregates to reduce the environmental problem. Moreover, the application of C&D materials can mitigate the shortage problems of quality natural materials, with the advantage of a lower carbon footprint compared to the ordinary aggregates.

Reclaimed asphalt pavement (RAP), crushed brick (CB), and recycled concrete aggregate (RCA) are the major streams of C&D materials in pavement engineering applications. CB is a by-product of building demolition and is composed of approximately 70% brick and 30% other components such as cement. For pavement engineering applications, the California bearing ratio (CBR) and Los Angeles abrasion loss of CB material were found to be sufficient to satisfy the minimum requirement for the sub-base layer specified by the local road authority. CB has been recommended for usage in pavement sub-base applications with a moisture ratio of around 65% because the strength of CB decreases with further increases in the moisture ratio beyond 65%. CB can be mixed with the other durable aggregates in order to improve the engineering properties and durability [12–16].

RAP is the waste product associated with the demolished asphalt concrete of the wearing of a pavement surface. Previous research on C&D materials revealed that RAP aggregate was suitable for pavement bases. The shear strength under static loading of pure RAP is similar to loose sand. However, due to its very low cohesion values, the resilience properties under the cyclic loading of RAP could not be determined. The RAP aggregate has a more pronounced performance when stabilized with cement. The cement-stabilized RAP has dominant resilient properties that can meet the minimum requirements of the local road authority [17–20].

Recycled concrete aggregate (RCA) is the by-product of concrete structure demolition in the aggregate form after the crushing process. RCA has sufficient engineering properties and superior deformation responses compared to other C&D materials and thus can be used for the sustainable construction of unbound pavement layers. In addition, pavement base layers containing RCA materials have sufficient durability against extreme weathering, such as wet–dry and freeze–thaw cycles [21–24]. As such, the construction of geothermal pavements with C&D wastes such as CB, RAP, and RCA further enhances the sustainability of the system while maintaining the structural integrity of the pavement.

Previous research has studied the effects of C&D materials on geotechnical and environmental properties [25–30]. However, research on the influence of C&D materials on geothermal systems is limited to date. A geothermal system is an advancement in renewable energy resources for heating and cooling systems. For example, a shallow

geothermal heat pump system, which consists of ground heat exchangers, is an effective system with regard to transferring the thermal energy between the ground and the heat pump to distribute the thermal energy. The pipes in a geothermal pavement system can be installed in asphalt concrete pavements to collect thermal energy, where it is characterized as an asphalt solar collector system. The energy from the asphalt solar collector system can be used effectively for the heating and cooling system of a building by storing energy in the ground. In addition to the energy collection, an asphalt solar collector system can effectively reduce pavement surface temperatures. The pipe system of an asphalt solar collector is commonly installed at a shallow depth in the pavement in order to prevent cracks in the asphalt layer due to the stress concentration around the pipe [25–30].

Based on the published literature [27–30], the pipe system of a geothermal pavement system can be installed in the base layer to minimize construction and maintenance costs. A geothermal pavement system, comprising a pipe system formed by a number of pipe circuits (for redundancy) in the base layer to collect the thermal energy, is an advancement in renewable energy resources for generating electricity as an alternative to the conventional power generation for both heating and cooling systems. For example, a shallow geothermal heat pump system, which consists of ground heat exchangers, is an effective system with regard to transferring thermal energy between the ground and the heat pump to distribute the thermal energy [25–27]. If any of the redundant pipe circuits experience leaks or ruptures during the pavement's lifetime, that particular circuit is closed off, and the system continues in operation until the pipe is repaired or continues at a slightly reduced efficiency if the circuit is abandoned. Further details on geothermal design and operation can be found in the literature [25,26]. In addition to heating and cooling applications, the collected energy from the geothermal pavement system may be able to generate electricity for the buildings in the vicinity of the road [9,27–34].

The incorporation of C&D materials in the pavement base layer of geothermal pavements further enables a lower-carbon pavement system. C&D materials were established as mainstream pavement base materials in Australia after an earlier benchmarking of their performance against quarry aggregates indicated they provide equivalent or superior performance. C&D materials have also been incorporated into road authority standards, enabling their usage in pavement base applications. However, it is important to understand how the thermal and mechanical properties of C&D materials affect the performance of geothermal pavements [35]. To date, no known studies have investigated the long-term deformation responses of geothermal pavements under traffic loading. The effect of pipe inclusion on the deformation and strength properties of pavement materials is also of great importance. In addition to mechanical properties, the effects of different parameters such as pipe material and flow rate on the thermal performances of geothermal pavements should be investigated.

This research study attempted to investigate the long-term mechanical properties of geothermal pavements constructed with C&D materials in pavement bases using experimental testing, prototype testing, and numerical methods. Permanent strain development due to repetitive traffic loading is a long-term response to a time-dependent process [16]. The accumulated permanent strain increases with an increasing number of vehicle passes. In this work, the permanent deformation responses of geothermal pavements were characterized using a combination of physical testing and numerical simulations. Laboratory repeated-load triaxial (RLT) and repeated-load California bearing ratio (CBR) testing was undertaken to analyze the time-dependent evolution response toward permanent deformation, the resilient moduli, and the strength responses of the C&D materials with pipes. A small-scale prototype system was used to evaluate the short- and long-term thermal performances of the geothermal pavements. Based on the experimental results, a numerical model (which also considered the different target levels of stresses of the geothermal pavements) was developed to investigate the effects of influential parameters on the thermal performances of the systems in the long term. The outcomes of this research, as evidenced by the extensive experimental testing, prototype testing, and numerical modeling, will

build further confidence in using C&D materials in the construction of new geothermal pavements and will assist in enabling their future commercialization.

2. Materials and Methods

2.1. Experimental Investigation

Recycled concrete aggregate (RCA), crushed brick (CB), and reclaimed asphalt pavement (RAP) were used for the deformation analysis of the prototype geothermal pavement system under long-term cyclic loads. These materials were collected from recycling sites across Victoria, Australia. The physical properties of the utilized C&D materials have been described in the published literature [9].

In this regard, a prototype square testing tank (50 cm × 50 cm) was designed to investigate the deformation responses of geothermal pavement under long-term cyclic loading conditions. A single pavement base layer with an approximate thickness of 40 cm and constructed with C&D materials was equipped with high-density polyethylene (HDPE) pipes with circulating fluid and was subjected to cyclic loading. The pipes were inserted approximately 10 cm into the RCA base. A multistage cyclic loading procedure consisting of 5 loading stages with 40,000 cycles (frequency = 1 Hz) in each stage was applied to the center of the pavement through a circular plate with a diameter of 10 cm. In total, 200,000 load cycles were applied to the geothermal pavements constructed with RCA, CB, and RAP. The applied cyclic stress had a haversine shape and varied between 150 kPa and 550 kPa in 100 kPa intervals, according to Austroads repeated-load triaxial test method AG:PT/T053 [36], to evaluate the long-term performance of the system under a wide range of stress levels. The testing started at room temperature, and the temperature was changed to 45 °C after approximately 30,000 load cycles. Figure 1 presents the experimental setup for long-term physical testing.

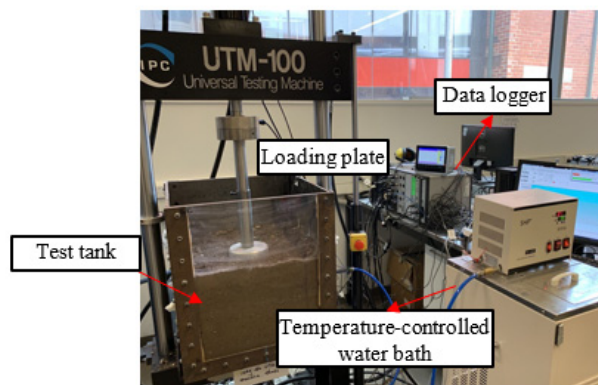


Figure 1. Prototype testing setup.

A series of repeated-load triaxial (RLT) tests were undertaken to investigate the effect of pipe inclusion on the deformation behavior of the RCA samples, as RCA had more favorable deformation properties compared to the CB and RA, which were used in the long-term deformation assessment. Three types of pipes, including HDPE, polyethylene (PE), and copper, were inserted at two different depths within the compacted samples. The samples were prepared in 5 layers using a vibratory hammer at their optimal moisture content (OMC) to obtain a compaction degree equal to at least 98% of the maximum dry density (MDD). The pipes were positioned in a mold after compaction of the 3rd (case 1) and 4th (case 2) layers. A three-stage RLT testing procedure consisting of constant confining stress at 50 kPa and deviator stresses equal to 250 kPa, 350 kPa, and 450 kPa was applied to the samples according to Austroads repeated-load triaxial test method AG:PT/T053 [36]. Each stage included 10,000 cycles of cyclic loads with loading and resting periods of 1 s and 2 s, respectively. The resilient moduli (MR) of the samples were characterized by applying 65 various combinations of confining and deviator stresses as per the Australian standard.

To further investigate the effect of pipe inclusion on the deformation of the RCA, repeated-load California bearing ratio (RL-CBR) tests were undertaken. The procedure adopted for the RL-CBR tests was similar to those used by Araya et al. in 2010 [37] and Haghghi et al. in 2018 [38], with some modifications. The samples were loaded using the loading plunger at a constant rate of 1 mm/min, and the forces and corresponding deformations were recorded. Once the sample reached a deformation value of 5 mm, the peak load was recorded, and the loading plunger was unloaded to 0.05 kN (seating load) to complete the first cycle. The loading was repeated for 10 cycles, where the majority of deformations tended to become recoverable, to complete the first stage of the RL-CBR testing. Upon the completion of the first stage, the peak load for the first stage was increased by 30% and 10 cycles were applied to the samples. Similarly, the peak load of the second stage was increased by 30% in the third stage of the RL-CBR test, and the increased load was applied for 10 further cycles. Figure 2 shows the sample preparation for the RL-CBR tests and a prepared sample for RLT testing.



Figure 2. (a–c) RL-CBR sample preparation with HDPE, PE, and copper pipes. (d) Prepared RLT sample with a copper pipe.

2.2. Thermal Performance

A small-scale prototype pavement system measuring 300 mm × 300 mm × 170 mm was used to evaluate the thermal performance of the system. The geothermal pavement system was composed of a 50 mm asphalt layer over a 100 mm C&D base. A similar setup was previously used in [7]. A serpentine HDPE pipe with a diameter of 20 mm was inserted 2 cm below the interface between the C&D base layer and the asphalt concrete surface layer. Four infrared heating lamps were used to heat the asphalt surface, and temperature sensors were placed on the surface of the system. A constant flow rate of 1000 mL/min was used in the experiments. The experiments started with heating the pavement surface for more than 7 h without the circulation of water in the system (case 1) and simultaneous surface heating and water circulation in the system (case 2). Figure 3 presents the test setup and the positioning of the HDPE pipe within the pavement system.

A numerical model was subsequently developed using the computational fluid dynamics code FLUENT to assess the effects of pipe materials and flow rates on the pavement surface temperature. The three main heat transfer mechanisms in pavements are radiation, conduction, and convection. A geothermal pavement system has interactions with the surrounding environment. It was necessary to define appropriate boundary conditions to obtain accurate and precise results. The main heat transfer mechanisms on the pavement surface are radiative and convective heat transfer. The energy equation can be defined as follows [4,6]:

$$-k \frac{\partial T}{\partial t} = a_s q_s + \varepsilon \sigma (T_{sky}^4 - T^4) + h(T_a - T) \quad (1)$$

where a_s is the absorptivity; q_s is the solar irradiation; ε represents emissivity; σ is the Stephan–Boltzmann constant (5.669×10^{-8}); and T , T_{sky} , and T_a are the surface temperature, sky temperature, and air temperature, respectively. Here, T_a was measured using a temperature sensor, and it was assumed that $T_{sky} = T_a$ [37]. The convective heat transfer coefficient (h) was calculated to be equal to 5.6 (wind speed = 0), according to the empir-

ical Bentz model, as the experiments were undertaken in a laboratory with a controlled environment.

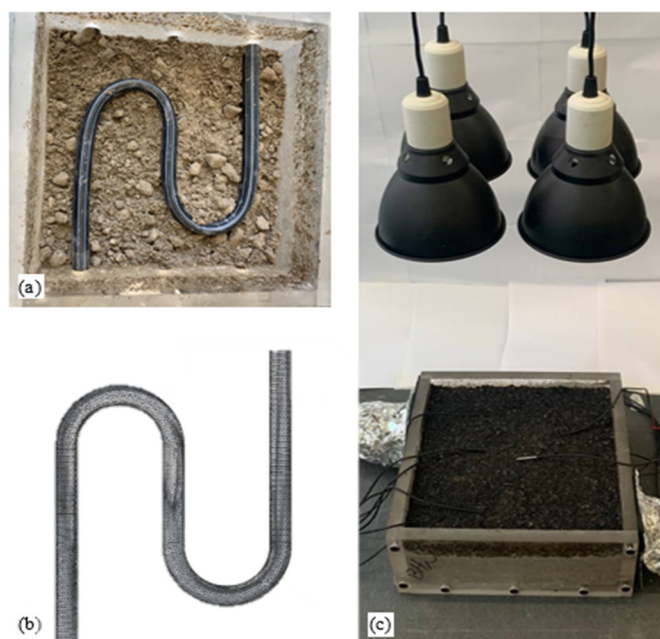


Figure 3. (a) Layout of HDPE pipe within the RCA base. (b) Plan of the prototype system in the numerical simulations. (c) Setup of experiments.

The thermal conductivity of the asphalt concrete and RCA were obtained using the divided bar method [7,9]. Table 1 summarizes the thermal properties of the materials used in the numerical simulations. To control the entry of the flow and the flow rate during simulations, a user-defined function was used. The inlet velocity for the validation of the numerical model was the same as in the experiments (1000 mL/min), and the water had a constant temperature of 22 °C. Other flow rates (500 mL and 2000 mL/min) were also considered to evaluate their effects on the system's performance. Similar to the experiments, two cases were considered in the numerical simulations: case 1, where there was no circulation of water and the pavement was under constant heating for more than 7 h, and case 2, where the heating and flow circulation started simultaneously.

Table 1. Thermal and physical properties of materials used in numerical simulations (data from Arulrajah et al. (2021) [7] and Ghorbani et al. (2021a) [9]).

Material	λ (W/(m.K))	C_p (J/(kg.K))	ρ (kg/m ³)
Asphalt	1.73	870	2350
RCA	1.65	1050	2200
Water	0.614	4187	999
HDPE pipe	0.50	2000	970
Copper pipe	387	381	8978

3. Results

3.1. Experimental Characterization

Figure 4 presents the relationship between permanent deformation and the number of cycles under the long-term cyclic loading of C&D materials using a prototype geothermal pavement tank test. RCA exhibited a stable response and a negligible increase in permanent deformations with load cycles. The maximum permanent deformation of the geothermal pavement constructed with RCA was approximately 2.5 mm. CB showed a considerable increase in the permanent deformation at the initial cycles of each stage, followed by

a consistent increase in the permanent deformations with the number of cycles. The maximum permanent deformation of the geothermal pavement with CB was approximately 16.3 mm, which was considerably higher than that of the RCA. On the other hand, RAP exhibited unstable behavior, even in the initial loading stage, which resulted in failure in the second stage of the test. Based on the above discussion, RCA was selected as the primary material for further testing due to its stable behavior and small deformations under long-term cyclic loads.

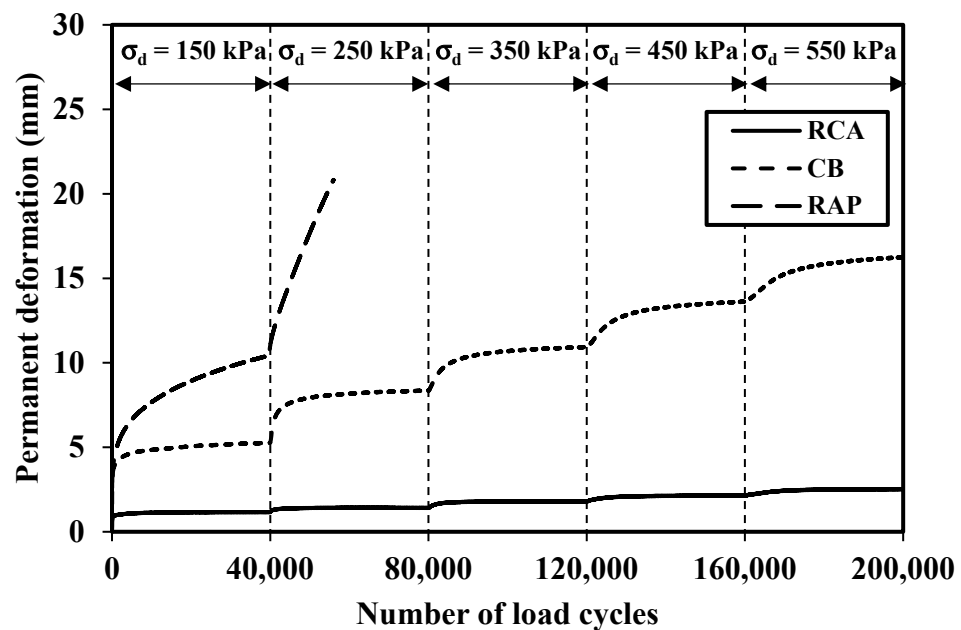


Figure 4. The permanent deformation responses of geothermal pavement systems under long-term cyclic loading.

Figure 5 shows a schematic of the shakedown theory and the relationship between permanent deformation and the number of cycles in the long-term cyclic loading tests of the RCA samples with different pipe types and two pipe inclusion depths. The permanent strain increased with an increase in the number of cycles for all C&D materials. At the same number of cycles, the material with a higher resilient response exhibited a lower permanent strain. Based on the shakedown theory, the unbound granular material behavior under repetitive stress could be classified as plastic shakedown (range A), plastic creep (range B), and incremental collapse (range C), as presented in Figure 5a. For range A, the material had a relatively large permanent strain increment in the primary stage and exhibited an entirely resilient response (stopped accumulating plastic strain) in the secondary stage. For range B, the material experienced a large permanent strain increment in the primary stage, and the rate of permanent strain increased slower in the secondary stage. For range C, the large amount of permanent material strain increased rapidly in the primary stage, which ultimately caused failure in the secondary stage due to the accumulated permanent strain [5].

It was evident that the RCA material with and without pipe experienced a small permanent strain increment in the secondary stage (Figure 5b). Therefore, the permanent strain responses of the studied material were classified as range A, which can be used as pavement material. As noted in the figure, regardless of the pipe type and inclusion depth, the permanent strains of all samples were lower than 0.86%. That is, all samples exhibited small permanent strain values and stable behavior under the applied stress combinations. A closer observation of the results indicated that the inclusion of plastic pipes (HDPE and PE) increased the permanent strain of the RCA, and the samples with HDPE pipes showed slightly higher permanent strain values than those with PE pipes. However, at the same temperature, the inclusion of copper pipes had a negligible effect on the permanent strain

values. The permanent strain trends for the RCA samples with copper pipes were relatively similar to the RCA samples. These results can be attributed to the higher stiffness of copper pipes compared to HDPE and PE pipes. The position of the pipe resulted in the difference in permanent strain. The influence of the pipe-embedded layer could be observed. In case 1, pipe installation had a lower permanent strain than case 2. It can be interpreted that the deeper pipe-embedded layer could reduce the stress concentration on the pipe, thereby lowering the permanent strain at the same number of cycles. Nevertheless, the results indicate that, given the stress levels of the unbound base layer, pipes can be inserted into the unbound base layer without worrying about excessive deformations.

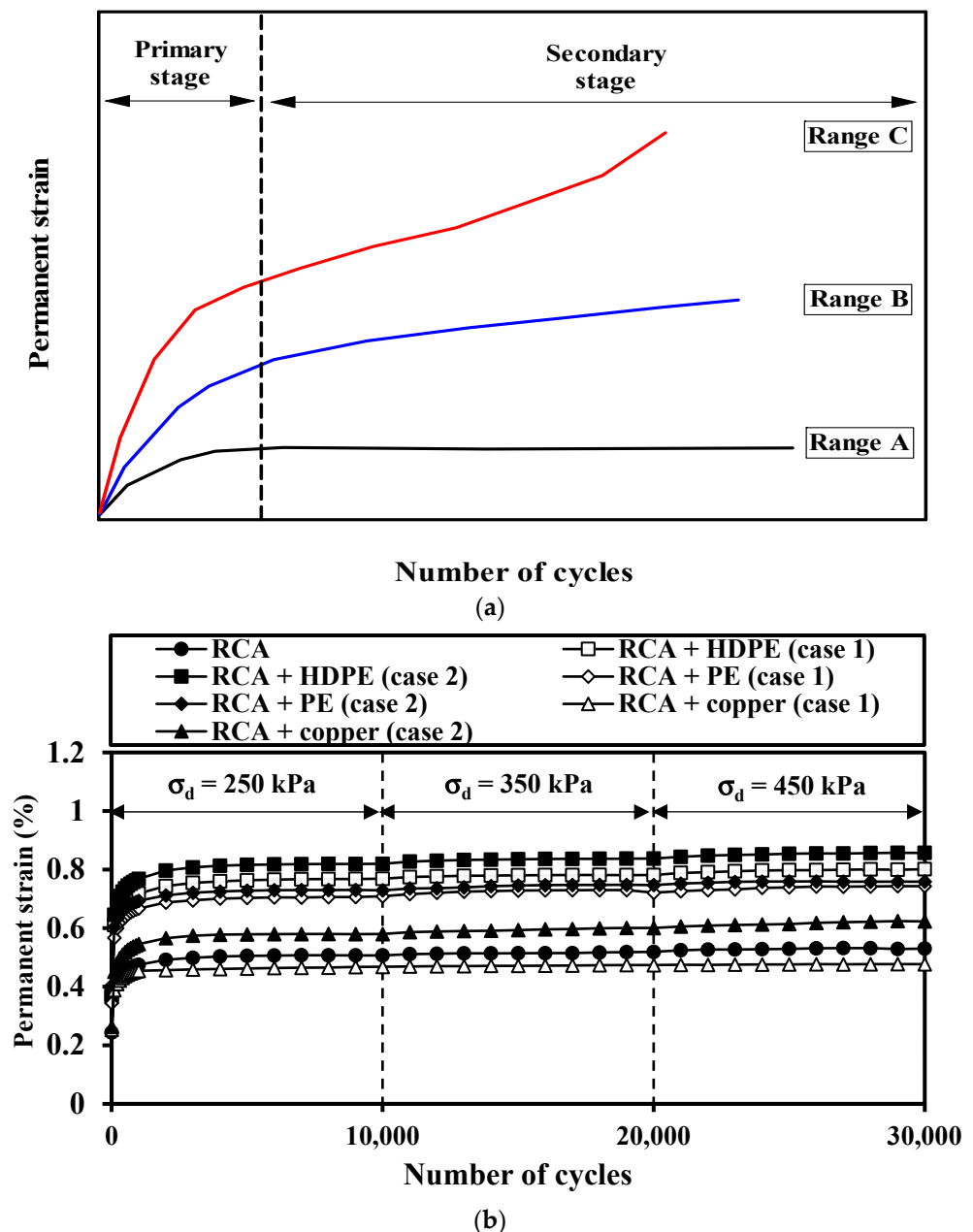


Figure 5. (a) Schematic of shakedown theory and (b) permanent strain responses of samples with the inclusion of pipes.

Figure 6 presents the relationship of the resilient moduli versus the stage numbers of RCA samples with different pipe inclusions. At the same stage number, the MR of samples slightly decreased with the inclusion of pipes. Due to the stiffness of cop-

per, the RCA + copper sample exhibited MR values equivalent to those of RCA. Meanwhile, the RCA + PE and RCA + HDPE samples exhibited slightly lower MR values than RCA + copper and RCA because of the lower stiffness of the PE and HDPE pipes. The pipe-embedded layer slightly influenced the MR values at a high stage number, where case 2 pipe installations had slightly lower MR values than case 1 installations for all pipe types.

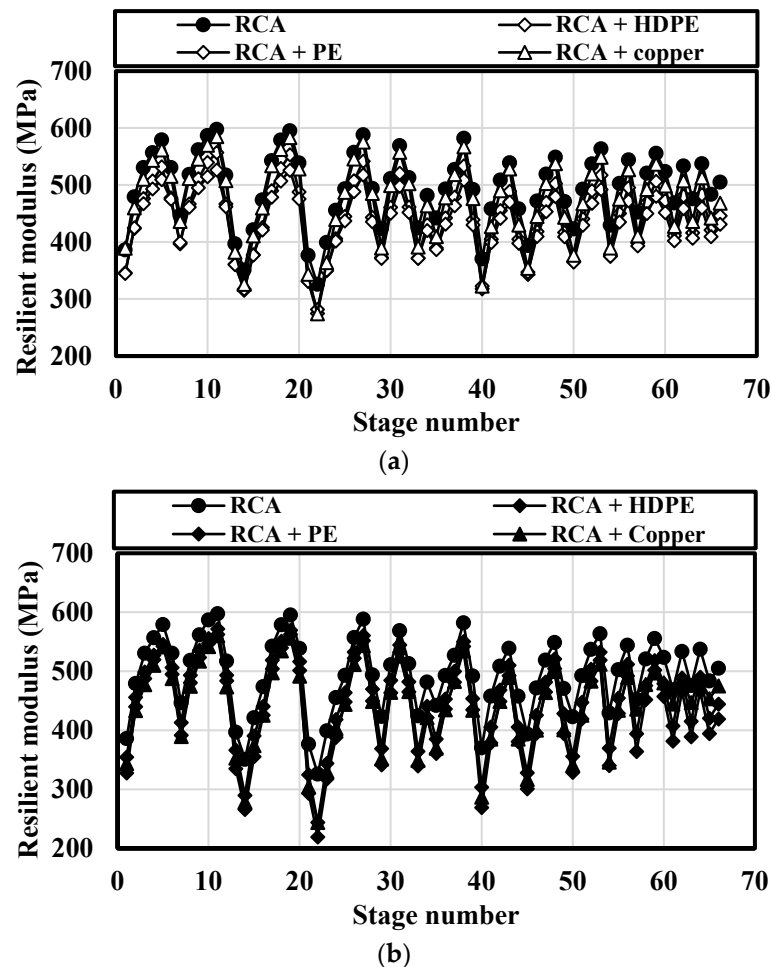


Figure 6. Resilient modulus responses of samples with pipe inclusion: (a) case 1 and (b) case 2.

The RL-CBR test was performed on unsoaked RCA samples with different pipe types. The load–deformation behavior of samples under the three stages of RL-CBR is presented in Figure 7. As noted in this figure, the peak loads of the first stage for the RCA, RCA + HDPE, RCA + PE, and RCA + copper samples were 27.1 kN, 21.7 kN, 27.1 kN, and 30.0 kN, respectively. The inclusion of the HDPE pipe reduced the stiffness of the RCA + HDPE mix and resulted in a decrease in the peak load. On the other hand, the high stiffness of the copper pipe improved the strength of the mix and resulted in a higher peak load. Another notable observation was the higher deformation of RCA + copper compared to the other mixes. While the higher peak loads could be the reason for high values of the deformation for the RCA + copper mix, the brittle behavior of the copper pipe once the failure point was reached would be another important contributing factor. This was evident in the third stage of the RL-CBR test, where the applied load was beyond the capacity of the copper pipe and large deformations were observed. In other words, although copper pipes have better resistance against applied loads, they exhibit a brittle response when failure occurs.

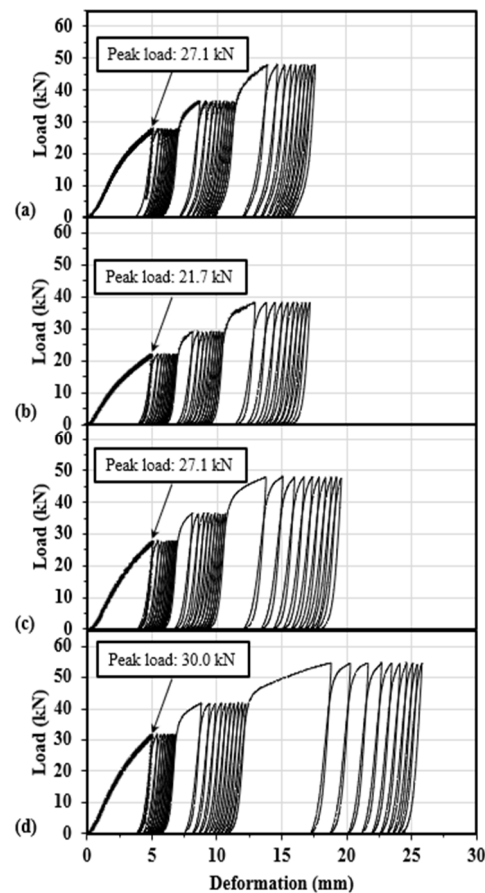


Figure 7. RL-CBR testing of (a) RCA, (b) RCA + HDPE, (c) RCA + PE, and (d) RCA + copper samples.

3.2. Numerical Simulation

Figure 8a shows the pavement surface temperature profiles obtained from experimental and numerical analyses. There was a consistent increase in the surface temperature with increasing time, with a higher rate of increase when there was no circulation in the system (case 1). For case 2, the initial increase in the surface temperature was followed by a decrease in the temperature accumulation rate, which indicated the efficiency of the system for reducing the surface temperature. The surface temperature stabilized and reached a constant value after almost 6 h of simultaneous heating and water circulation. Figure 8b presents the predicted temperatures from numerical simulations versus the experimental results, indicating that there was a reasonable agreement between the experimental results and the numerical simulation results.

The validated numerical model was subsequently used to investigate the effects of pipe materials and flow rates on the performance of the system. Figure 9a presents the surface temperature profiles for different flow rates (500 mL/min to 2000 mL/min) and pipe materials (HDPE and copper). As noted, the flow rate had a negligible effect on the surface temperature. For the HDPE pipe, increasing the flow rate from 500 mL/min to 2000 mL/min reduced the surface temperature by approximately 1.3%. Similar results were obtained for the copper pipes, which indicated that the flow rate was not a governing factor affecting the surface temperature. At a constant flow rate of 2000 mL/min, using copper pipe resulted in an approximately 4% further decrease in the surface temperature. In addition, varying the flow rate during testing (Figure 9b) also had small effects on the surface temperature profile.

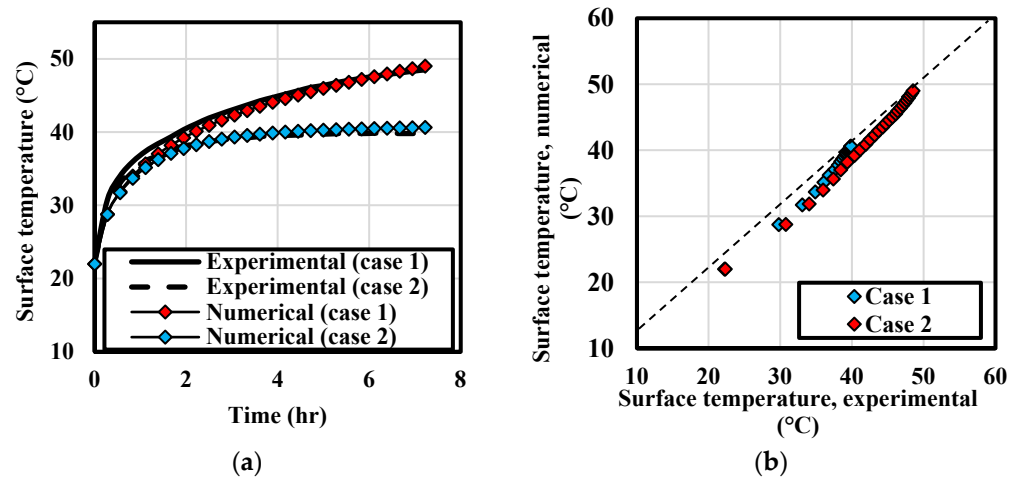


Figure 8. (a) The surface temperature profiles in the experimental and numerical analyses. (b) Comparison of experimental and predicted temperatures.

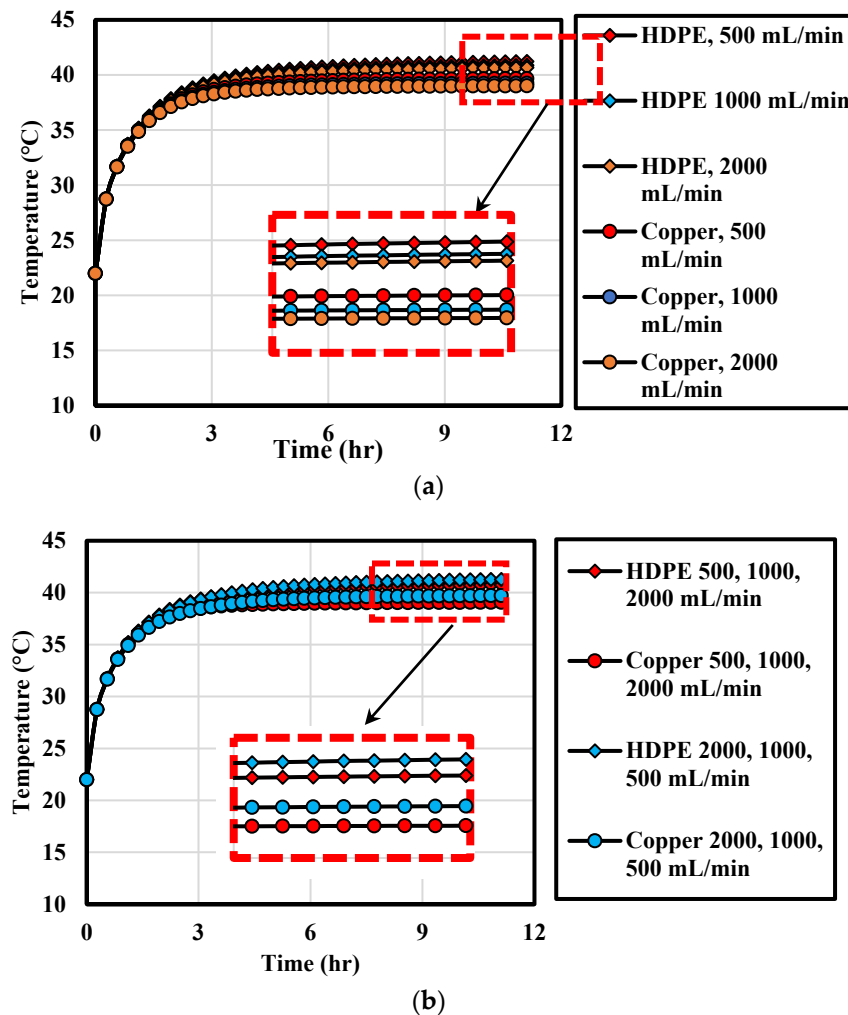


Figure 9. Effects of (a) constant flow rates and pipe materials and (b) varied flow rates and pipe materials on the surface temperature profile.

4. Conclusions

This research evaluated the deformation, strength, and thermal performance of geothermal pavements constructed with C&D materials. The following significant findings can be summarized from this research:

1. The deeper pipe-embedded layer can reduce the stress concentration on the pipe, leading to lower permanent deformation after the same number of cycles. The inclusion of pipes in the pavement base layer was found to have negligible detrimental effects on the deformation behavior of RCA. Regardless of the pipe type and inclusion depth, the permanent strain values of all RCA samples were lower than 0.86%. It can be concluded that the pipes can be inserted in unbound granular layers without causing excessive deformations.
2. Due to the higher permanent deformation, the MR of RCA samples slightly decreased with the inclusion of pipes. The RCA + copper sample exhibited MR values equivalent to those of RCA because of its adequate stiffness, and the RCA + PE and RCA + HDPE samples exhibited slightly lower MR values. Similar to the permanent deformation results, the inclusion of the pipes had no significant detrimental effects on the resilient modulus of RCA.
3. The results of the RL-CBR test indicated that the inclusion of the HDPE pipe reduced the peak load of the stiffness of the RCA + HDPE mix due to the loss of stiffness. On the other hand, the high stiffness of the copper pipe improved the strength of the mix and resulted in a higher peak load. The total deformation for the RCA + copper mix was the highest due to the brittle response of the copper pipe and the significant deformations once the failure point was reached under monotonic loading.
4. A numerical analysis was developed to evaluate the effects of pipe materials and flow rates on the surface temperature. The numerical model was calibrated using the experimental data. The parametric study indicated that the flow rate had negligible effects on the surface temperature for both the HDPE and copper pipes. Copper pipes were slightly more efficient in reducing the surface temperature compared to HDPE pipes. At a constant flow rate of 2000 mL/min, using a copper pipe resulted in an approximately 4% further decrease in the surface temperature compared to the HDPE pipe. It was also noted that varying flow rates during testing had small effects on the surface temperature profile.
5. The installation of plastic pipes (HDPE and PE) and copper pipes in the unbound base layer can effectively reduce the pavement's surface temperature without a large effect of excessive deformation. At the same temperature, the copper pipe had a high potential to transfer the surface heat with lower permanent strain compared to the RCA without a pipe. Meanwhile, the plastic pipes caused slightly higher permanent deformation than the RCA layer without a pipe and had a slightly lower potential to reduce the surface temperature compared to RCA with a copper pipe but at a much-reduced material cost.

Author Contributions: Conceptualization, B.G. and A.A.; methodology, B.G. and A.A.; software, B.G.; validation, B.G., A.A., G.A.N. and S.H.; formal analysis, B.G. and A.B.; investigation, B.G. and A.A.; resources, A.A., G.A.N. and S.H.; data curation, B.G. and A.A.; writing—original draft preparation, B.G., A.A., S.H. and A.B.; writing—review and editing, B.G., A.A., S.H. and A.B.; visualization, B.G., A.A. and G.A.N.; supervision, A.A., G.A.N. and S.H.; project administration, B.G. and A.A.; funding acquisition, A.A., G.A.N. and S.H. All authors have read and agreed to the published version of the manuscript.

Funding: This research was funded by the Australian Research Council's Linkage Projects funding scheme (project number LP200301154).

Institutional Review Board Statement: Not applicable.

Informed Consent Statement: Not applicable.

Data Availability Statement: Some or all data, models, or code that support the findings of this study are available from the corresponding author upon reasonable request. All data shown in the figures and tables can be provided upon request.

Acknowledgments: This research was supported by the Australian Research Council's Linkage Projects funding scheme (project number LP200301154).

Conflicts of Interest: The authors declare no conflict of interest.

References

1. Pascual-Muñoz, P.; Castro-Fresno, D.; Serrano-Bravo, P.; Alonso-Estébanez, A. Thermal and hydraulic analysis of multilayered asphalt pavements as active solar collectors. *Appl. Energy* **2013**, *111*, 324–332. [\[CrossRef\]](#)
2. Chiarelli, A.; Dawson, A.; Garcia, A. Field evaluation of the effects of air convection in energy harvesting asphalt pavements. *Sustain. Energy Technol. Assess.* **2017**, *21*, 50–58. [\[CrossRef\]](#)
3. Ghorbani, B.; Arulrajah, A.; Narsilio, G.; Horpibulsuk, S. Experimental and ANN analysis of temperature effects on the permanent deformation properties of demolition wastes. *Transp. Geotech.* **2020**, *24*, 100365. [\[CrossRef\]](#)
4. Guldentops, G.; Nejad, A.M.; Vuye, C.; Rahbar, N. Performance of a pavement solar energy collector: Model development and validation. *Appl. Energy* **2016**, *163*, 180–189. [\[CrossRef\]](#)
5. Mallick, R.B.; Chen, B.-L.; Bhowmick, S. Harvesting heat energy from asphalt pavements: Development of and comparison between numerical models and experiment. *Int. J. Sustain. Eng.* **2012**, *5*, 159–169. [\[CrossRef\]](#)
6. Zaim, E.H.; Farzan, H.; Ameri, M. Assessment of pipe configurations on heat dynamics and performance of pavement solar collectors: An experimental and numerical study. *Sustain. Energy Technol. Assess.* **2020**, *37*, 100635. [\[CrossRef\]](#)
7. Arulrajah, A.; Ghorbani, B.; Narsilio, G.; Horpibulsuk, S.; Leong, M. Thermal performance of geothermal pavements constructed with demolition wastes. *Geomech. Energy Environ.* **2021**, *28*, 100253. [\[CrossRef\]](#)
8. Gabr, A.; Cameron, D. Properties of recycled concrete aggregate for unbound pavement construction. *J. Mater. Civ. Eng.* **2012**, *24*, 754–764. [\[CrossRef\]](#)
9. Ghorbani, B.; Arulrajah, A.; Narsilio, G.; Bo, M. Thermal and mechanical properties of demolition wastes in geothermal pavements by experimental and machine learning techniques. *Constr. Build. Mater.* **2021**, *280*, 122499. [\[CrossRef\]](#)
10. Yaghoubi, E.; Disfani, M.M.; Arulrajah, A.; Kodikara, J. Development of a void ratio-moisture ratio-net stress framework for the prediction of the volumetric behavior of unsaturated granular materials. *Soils Found.* **2019**, *59*, 443–457. [\[CrossRef\]](#)
11. Sustainability Victoria. *Victorian Recycling Industries Annual Report 2008–2009*; Sustainability Victoria: Melbourne, VIC, Australia, 2010; ISSN 1836-9902.
12. Jankovic, K.; Nikolic, D.; Bojovic, D. Concrete paving blocks and flags made with crushed brick as aggregate. *Constr. Build. Mater.* **2012**, *28*, 659–663. [\[CrossRef\]](#)
13. Gayarre, F.L.; López-Colina, C.; Serrano, M.A.; López-Martínez, A. Manufacture of concrete kerbs and floor blocks with recycled aggregate from C and DW. *Constr. Build. Mater.* **2013**, *40*, 1193–1199. [\[CrossRef\]](#)
14. Liu, H.J.; Li, P.X.; Cao, S.G.; Zhao, F.Q. Preparation of high-performance brick from construction and demolition waste. In *Advanced Materials Research*; Trans Tech Publications Ltd.: Wollerau, Switzerland, 2012; Volume 391, pp. 180–183.
15. Gregory, R.J.; Hughes, T.G.; Kwan, A.S.K. Brick recycling and reuse. In *Proceedings of the Institution of Civil Engineers-Engineering Sustainability*; No. 3; Thomas Telford Ltd.: London, UK, 2004; Volume 157, pp. 155–161.
16. Yaghoubi, E.; Sudarsanan, N.; Arulrajah, A. Stress-strain response analysis of demolition wastes as aggregate base course of pavements. *Transp. Geotech.* **2021**, *30*, 100599. [\[CrossRef\]](#)
17. Taha, R.; Al-Harthy, A.; Al-Shamsi, K.; Al-Zubeidi, M. Cement stabilization of reclaimed asphalt pavement aggregate for road bases and subbases. *J. Mater. Civ. Eng.* **2002**, *14*, 239–245. [\[CrossRef\]](#)
18. Hoyos, L.R.; Puppala, A.J.; Ordonez, C.A. Characterization of cement-fiber treated reclaimed asphalt pavement aggregates: Preliminary investigation. *J. Mater. Civ. Eng.* **2011**, *23*, 977–989. [\[CrossRef\]](#)
19. Puppala, A.J.; Hoyos, L.R.; Potturi, A.K. Resilient moduli response of moderately cement-treated reclaimed asphalt pavement aggregates. *J. Mater. Civ. Eng.* **2011**, *23*, 990–998. [\[CrossRef\]](#)
20. Yaghoubi, E.; Ahadi, M.R.; Sheshpoli, M.A.; Pahlevanloo, H.J. Evaluating the performance of hot mix asphalt with reclaimed asphalt pavement and heavy vacuum slops as rejuvenator. *Int. J. Transp.* **2013**, *1*, 115–124.
21. Melbouci, B. Compaction and shearing behavior study of recycled aggregates. *Constr. Build. Mater.* **2009**, *23*, 2723–2730. [\[CrossRef\]](#)
22. Sivakumar, V.; McKinley, J.D.; Ferguson, D. Reuse of construction waste: Performance under repeated loading. *Proc. Inst. Civ. Eng. Geotech. Eng.* **2004**, *157*, 91–96. [\[CrossRef\]](#)
23. Azam, A.; Cameron, D. Geotechnical properties of blends of recycled clay masonry and recycled concrete aggregates in unbound pavement construction. *J. Mater. Civ. Eng.* **2013**, *25*, 788–798. [\[CrossRef\]](#)
24. Ghorbani, B.; Arulrajah, A.; Narsilio, G.; Horpibulsuk, S.; Leong, M. Resilient moduli of demolition wastes in geothermal pavements: Experimental testing and ANFIS modelling. *Transp. Geotech.* **2021**, *29*, 100592. [\[CrossRef\]](#)
25. Remund, C.; Carda, R.; Rawlings, P.; Bose, J. *Ground Source Heat Pump Residential and Light Commercial Design and Installation Guide*; International Ground Source Heat Pump Association, Oklahoma State University: Stillwater, OK, USA, 2009.

26. Gu, X.; Makasis, N.; Motamedi, Y.; Narsilio, G.A.; Arulrajah, A.; Horpibulsuk, S. Geothermal pavements: Field observations, numerical modelling and long-term performance. *Géotechnique* **2022**, *72*, 832–846. [[CrossRef](#)]
27. Dincer, I. Renewable energy and sustainable development: A crucial review. *Renew. Sustain. Energy Rev.* **2000**, *4*, 157–175. [[CrossRef](#)]
28. Brandl, H. Energy foundations and other thermo-active ground structures. *Géotechnique* **2006**, *56*, 81–122. [[CrossRef](#)]
29. Laloui, L.; Di Donna, A. Understanding the behaviour of energy geo-structures. In *Proceedings of the Institution of Civil Engineers-Civil Engineering*; Thomas Telford Ltd.: London, UK, 2011.
30. Loveridge, F.; McCartney, J.S.; Narsilio, G.A.; Sanchez, M. Energy geostructures: A review of analysis approaches, in situ testing and model scale experiments. *Geomech. Energy Environ.* **2020**, *22*, 100173.
31. Amatya, B.L.; Soga, K.; Bourne-Webb, P.J.; Amis, T.; Laloui, L. Thermo-mechanical behaviour of energy piles. *Géotechnique* **2012**, *62*, 503–519. [[CrossRef](#)]
32. Pan, P.; Wu, S.; Xiao, Y.; Liu, G. A review on hydronic asphalt pavement for energy harvesting and snow melting. *Renew. Sustain. Energy Rev.* **2015**, *48*, 624–634. [[CrossRef](#)]
33. Van Bijsterveld, W.; De Bondt, A. Structural aspects of asphalt pavement heating and cooling systems. In *Proceedings of the 3rd International Symposium on 3D Finite Element Modelling*, Amsterdam, The Netherlands, 2–5 April 2002.
34. He, X.; Abdelaziz, S.; Chen, F.; Yin, H. Finite element simulation of self-heated pavement under different mechanical and thermal loading conditions. *Road Mater. Pavement Des.* **2019**, *20*, 1807–1826. [[CrossRef](#)]
35. Bobes-Jesus, V.; Pascual-Muñoz, P.; Castro-Fresno, D.; Rodriguez-Hernandez, J. Asphalt solar collectors: A literature review. *Appl. Energy* **2013**, *102*, 962–970. [[CrossRef](#)]
36. AG:PT/T053; Determination of Permanent Deformation and Resilient Modulus Characteristics of Unbound Granular Materials under Drained Conditions. AustRoads: Sydney, NSW, Australia, 2000.
37. Araya, A.; Molenaar, A.; Houben, L. Characterization of unbound granular materials using repeated load CBR and triaxial testing. In *Paving Materials and Pavement Analysis*; Geotechnical Special Publication: Shanghai, China, 2010; pp. 355–363.
38. Haghghi, H.; Arulrajah, A.; Mohammadinia, A.; Horpibulsuk, S. A new approach for determining resilient moduli of marginal pavement base materials using the staged repeated load CBR test method. *Road Mater. Pavement Des.* **2018**, *19*, 1848–1867. [[CrossRef](#)]

Disclaimer/Publisher’s Note: The statements, opinions and data contained in all publications are solely those of the individual author(s) and contributor(s) and not of MDPI and/or the editor(s). MDPI and/or the editor(s) disclaim responsibility for any injury to people or property resulting from any ideas, methods, instructions or products referred to in the content.